Soil Dynamics and Earthquake Engineering 106 (2018) 14–30

Contents lists available at ScienceDirect

Soil Dynamics and Earthquake Engineering

journal homepage: www.elsevier.com/locate/soildyn

Historical development of friction-based seismic isolation systems

Paolo M. Calvi[a,*], Gian Michele Calvi[b]

[a] Department of Civil and Environmental Engineering, University of Washington, Seattle, WA, USA
[b] Scuola Universitaria Superiore, IUSS, Pavia, Italy

ARTICLE INFO

Keywords:
Base isolation
Friction pendulum
Multi-surface base isolation
Friction-based isolation systems, seismic protection, seismic performance

ABSTRACT

Base isolation has emerged as one of the most effective high-tech strategies for protecting infrastructure under seismic loading. This review paper discusses the historical development of friction-based seismic isolation systems, focusing on systems that have successfully been deployed and used as seismic safety measures for structures located in Europe. The conception and implementation of the Friction Pendulum system, the development of low friction materials and the effects of heating, contact pressure and velocity are discussed in light of past and recent numerical and experimental evidence. The merits of multiple surface devices, namely the Double Curvature Friction Pendulum and the Triple Friction Pendulum are also discussed, along with current knowledge and research gaps. Two European case studies, the Bolu Viaduct and the C.A.S.E. Project, are presented to illustrate that sliding base isolators can be used to meet otherwise unachievable design objectives. Finally, existing problems such as the response to high vertical accelerations, the potential for bearing uplift and the relevance of residual displacement are analyzed.

1. Introduction

In today's "performance-based" context, one effective way of protecting structures, and achieving a desired performance, is to mitigate the seismic demand on the system itself. To this end, one of the most promising solutions identified over the past few decades consists of installing low lateral stiffness devices, referred to as base isolators, beneath key supporting points of the structure. Base isolation has emerged as one of the most effective high-tech strategies for protecting infrastructures under seismic loading, both in the context of new construction, and in the retrofit of existing systems.

The goal of base isolation is normally to prevent the structure from damage, by shifting the fundamental period of a structure to the long period range and by absorbing the full displacement demand induced by seismic ground motions at the isolation layer. Isolating a structure results in a controlled structural response with reduced accelerations and lateral forces transmitted to the structure. The reduced seismic demand allows the superstructure to remain elastic, or nearly elastic, following a design level event. Furthermore, isolating a structure contributes to reducing the likelihood of damage to displacement sensitive and acceleration sensitive equipment, nonstructural components, and content.

Extensive research has been conducted on the topic of base isolation over the past few decades and the volume of information available in the literature has grown significantly, particularly in the last 15–20 years. To this end, a number of excellent reviews of aspects of the development, theory, and application of this technology can be found in the literature (e.g. [1–7] amongst many others).

However, given the amount of research available on base isolation, no single paper can provide an exhaustive literature review. Thus, authors are forced to either provide a general discussion of the topic, at the cost of providing limited details, or to provide detailed discussions, focusing only on selected issues. Furthermore, there is a steadily increasing production of new numerical and experimental literature, as a result of growing interest in the subject.

In this context, this review paper is dedicated to the historical development of friction-based seismic isolation systems, and particularly to systems that have successfully been deployed and used as seismic safety measures for structures located in Europe.

Though the concept of seismic isolation dates back more than one hundred years (e.g. [8,9]), modern friction sliding base isolators came about in the late 1980s and to date there are relatively few base-isolated structures in Europe.

While the concept of a friction-based isolating system was simple and attractive, the lack of a suitable restoring force delayed the implementation of sliding systems. Some attempts have been made at using a combination of flat sliders and "spring systems" that could serve as re-centering elements. One example can be found in the work of [10], who tested an isolation system utilizing a combination of elastomeric bearings and flat sliders. However, it was only after the

* Corresponding author.
E-mail address: pmc85@uw.edu (P.M. Calvi).

https://doi.org/10.1016/j.soildyn.2017.12.003
Received 16 August 2017; Received in revised form 20 October 2017; Accepted 3 December 2017
0267-7261/ Published by Elsevier Ltd.

conception of the modern Friction Pendulum ([11]) that sliding base isolators became a competitive alternative (and eventually a replacement) to more traditional solutions.

This paper begins by analyzing one rudimentary pendulum system proposed in 1909 (see [8]) to outline that the idea of isolating structures was conceived over 100 years ago but was unachievable because of technological limitations.

The modern Friction Pendulum is then introduced, focusing on a number of challenges that were gradually overcome. An extended discussion will be presented on problems associated with the performance of low friction materials and the effects of heating, contact pressure and velocity, in light of the most recent experimental evidence. Double Concave Friction Pendulum and Triple Friction Pendulum bearings are subsequently introduced. Their properties and benefits are discussed, and potential performance limitations and current knowledge gaps are outlined.

Two notable European case studies, the Bolu Viaduct (Turkey) and the C.A.S.E. Project (Italy), are used to illustrate the utilization of sliding base isolators as seismic solutions in two very different, but extremely challenging contexts.

Finally existing problems, such as the response to high vertical accelerations, the potential for bearing uplift and the relevance of residual displacement, are analyzed.

2. The “pendolo Viscardini” (1909)

In 1909, following the Messina earthquake, a friction-based isolation device was patented and proposed by Mario Viscardini (see Fig. 1 and [8] for a more detailed description). Viscardini states that perfect safety of a structure can be obtained allowing it to move as freely as possible with respect to the ground and affirms that such a performance can be obtained by introducing, at any contact point between soil and structure, a device consisting of a spherical body free to spin in any direction within two curved boxes, whose curvature assures a unique equilibrium position. He suggests to construct the building directly on such devices, using provisional shear keys, to be later removed.

This proposal induced discussions, followed by a firm decision condemning it, for reliability reasons. The burial stone came from Arturo Danusso [12], who wrote: we immediately understand that if we could practically put a house on springs, like an elegant horse-drawn carriage, an earthquake would come and go like a peaceful undulation for the happy inhabitants of that house, but concluded: I think that a certain practical sense of construction is sufficient by itself to dissuade from choosing mechanical devices to support stable houses.

From the patent drawings in Fig. 1, it is here assumed that the column side is 300 mm, and the spherical roller has a similar diameter. It is further assumed that the upper and lower spherical plates have a size of about 600 mm and their radius of curvature (r_s) is about 1000 mm. Considering reasonable values for contact pressure and sinkage depth, an estimate of the vertical load carrying capacity is about N = 1000 kN.

From these assumed values, it is straightforward to estimate the following properties:

$$\text{pendulum period of vibration: } T_p = 4\,\pi\sqrt{\frac{r_s}{g}} = 4s \tag{1}$$

$$\text{corresponding horizontal“stiffness” : } k_p = \frac{4\quad \pi^2 m}{T^2} = 250kN/m \tag{2}$$

The total displacement capacity can be assumed to be approximately equal to the difference in diameter between plates and spherical roller, i.e. Δ_u = 300 mm.

The calculation of the horizontal friction force V (at the onset of motion, at both points of contacts, upper and lower) can be determined from standard equations, such as:

$$\mathrm{V} = \frac{\mathrm{Nb}}{r} = \frac{1000\quad b}{150} = 0.67 - 3.3\,kN \tag{3}$$

Where b is a material-dependent constant and r is the radius of curvature of the spherical roller (previously assumed to be 150 mm).

The uncertainties associated with the properties of the materials available at the beginning of the twentieth century, allow only to brake the value of the constant b between 0.1 (e.g. for hardened steel used in spherical rollers) and 0.5 (e.g. for steel used in railway applications). However, this knowledge gap is not considered critical, since the resulting equivalent friction coefficient μ is always lower than 1%:

$$\mu = \frac{2\mathrm{V}}{N} = 0.13 - 0.67\,\% \tag{4}$$

Considering an average value of μ = 0.4%, the force-displacement relationship that may characterize the Viscardini's bearing is reproduced in Fig. 2. It is shown that the applied horizontal force, normalized with respect to the weight of the structure, corresponds to an acceleration of 0.4% g and 7.9% g, at the onset of motion and at the maximum displacement, respectively.

A cycle of this sort implies a very low equivalent damping (ξ_e), slightly higher than 3%:

$$\xi_e = \frac{2\mu\mathrm{N}}{\pi\mathrm{V}_{max}} = 3.2\% \tag{5}$$

The discussion presented above suggests that the Viscardini device might have had a vertical load carrying capacity and a horizontal displacement capacity acceptable for a reasonably wide scope of applications, while the shear force inducing movement was certainly too low, resulting in buildings oscillating under moderate winds and accidental actions. Perhaps, if not removed, the temporary shear keys that Viscardini recommended for construction purpose, could have worked as useful sacrificial links in case of an earthquake, but this option was

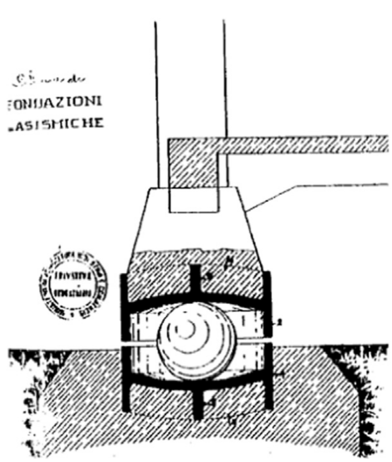

Fig. 1. The “Viscardini pendulum” (from [8]).

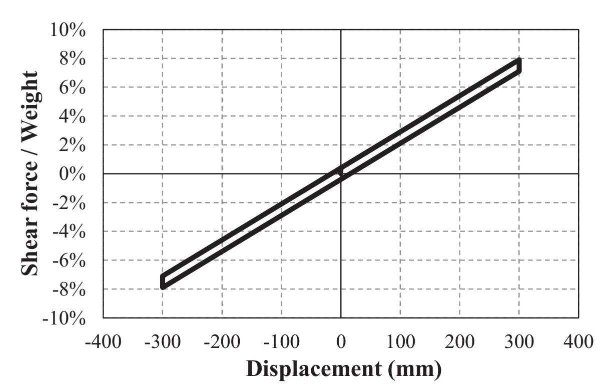

Fig. 2. Force-displacement hysteresis of Viscardini's device based on assumed values.

not explored. In addition, the moderate energy dissipation characterizing the device, would not have been effective in limiting the displacement demand in high seismicity regions.

Despite these flaws, the Viscardini device can possibly be regarded as one of the "ancestors" of the friction-based isolators which eighty years later would be further development and implemented.

To date, several systems of this "family" have been proposed, developed and implemented and thousands of tests have been performed worldwide. Within the European context, the most comprehensive review of experimental results pertaining to the friction properties of friction-based isolators was recently published by [13].

3. The friction pendulum system (1980s)

3.1. Conception and development

In the eighties, Victor Zayas revisited the idea of isolating buildings using devices based on friction and on the response of a pendulum (patent filed on Dec. 12, 1985 and published on Feb. 24, 1987, [14]).

The concept, design, modeling and testing of the system (referred to as "Friction Pendulum System") are described in a report published in 1987 [11] and in a journal paper published in 1990 [15]. Reading these documents is very interesting and should be done by anyone working on the subject of friction-based isolation.

The patent indicates ranges of application with velocities between 0 and 0.9 m/s, load bearing capacities between 7 and 210 MPa, friction coefficients between 5% and 20% and radii of curvature between 0.9 and 15 m. Several extremes of these very wide ranges were later shown to be technically impossible to meet, but the choice to consider this range may be justified by the desire to cover all possible applications and developments.

One of the original drawings included in the patent is reproduced in Fig. 3(a) (only the definition of three fundamental components is provided; more details can be found in the original document), which shows a device that looks quite different from the prototype later constructed and described in the report and in the paper, shown in Fig. 3(b). For instance, it is apparent from the comparison of the two figures that some problems related to stress concentration and deformation of concrete had been understood and addressed.

The report [11] contained evidence that has rarely been matched, in terms of quality and quantity. The tests were performed on a 6-dof shake-table, using four modifications of the isolated structure, with periods ranging from 0.23 and 0.99 s, and two different time scales of the ground motions, to simulate buildings with 4–30 stories. One of the specimens was further modified and included four levels of mass and stiffness eccentricity.

Five different sets of ground motion records were applied, with amplification factors ranging from 1 to 3, reaching maximum spectral accelerations between 0.32 g and 2.70 g.

The effects of vertical accelerations, including potential bearing uplift, were also addressed both numerically and experimentally.

The results were essentially in line with what today anyone would expect and predict, with a few points worth underlining:

a) The combined examination of the isolation system, the structure and the recorded total displacement, shows results that are in excellent agreement with what would have been suggested some twenty years later by [16]. Note that this is somewhat in contrast with the design approach for isolated structures used in the eighties (and nineties), which was based on the application of a modified acceleration response spectrum.
b) Surprisingly, the residual displacement was not investigated in detail considering the reported measurement magnitudes (never greater than 0.33 in, about 8 mm), much smaller than any reasonable residual inelastic drift. This is unfortunate, given that an experimental investigation of the same extent has never been repeated for base-isolated structures. In the meantime, the subject of residual displacement has gained importance, inspiring code limitations (e.g. on radius of curvature and energy dissipation capacity), not necessarily consistent with emerging evidence. More specifically, some recent experimental and numerical studies ([17–21]) demonstrated that the re-centering provision currently prescribed by the Eurocode ([22]) is not conservative for curved surface sliders, especially in presence of pulse-like earthquakes, and suggested that a more restrictive requirement should be adopted.
c) The theoretical coincidence of center of mass of the super-structure and center of stiffness of the isolation system (the "stiffness" of the pendulum is equal to borne weight divided by the radius of curvature) was demonstrated experimentally.
d) The effects of strong variation of the vertical load, due to the coupled response to horizontal and vertical actions, were shown to have limited effects on the horizontal displacement demand. However, the potential for significant modification of shear and bending acting on each column was not noted [23]: at the time, the use of isolation devices as local protection fuses, within the frame of capacity design, was not yet identified as one possible objective.
e) The low friction material used is simply described as PTFE, and it is indicated that the dynamic friction coefficient to be used in analytical simulations should be assumed equal to 8%. It is reported that this value "is higher than the quasi-static friction because the coefficient of friction of the bearing material increases with increased velocity". It is further stated that this is in agreement "with the known velocity dependent friction properties of PTFE bearing material". In fact, this is in contrast with the results of thousands of

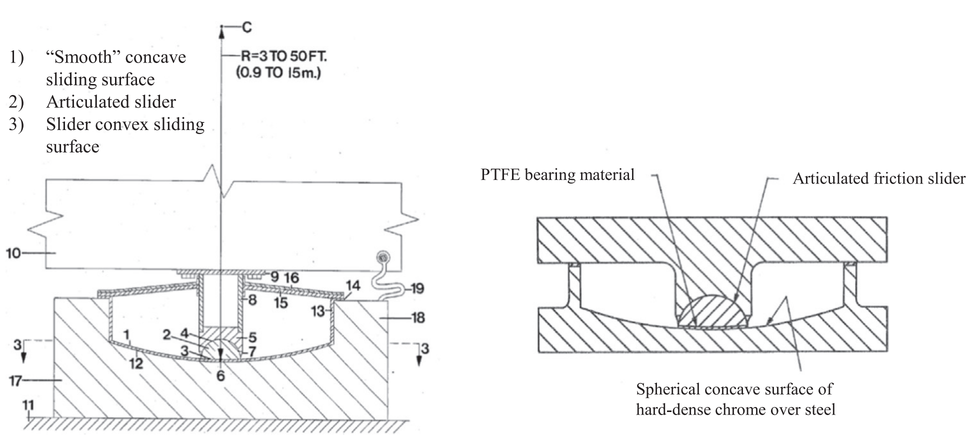

Fig. 3. The "friction pendulum system": (a) as depicted in [14]; (b) as depicted in [11] and [15].

tests performed on different low friction materials and isolation devices, which emphasize the exact opposite trend. This apparent contradiction is probably due to the combined effect of velocity and temperature: in general, higher temperatures favor a reduction of the friction coefficient values, and the temperature increases with velocity and pressure [13]. The resulting friction coefficient (in a specific point at a specific instant) results from the combined effect of velocity, pressure and temperature ([24], see also Section 4 of this paper) with global effects difficult to predict.

3.2. Further development and practical implementation

The Friction Pendulum (FP) system can meet a number of performance objectives but is particularly effective in the case of extremely large earthquake-induced displacement demand, for example in large bridge applications. This virtue has proved extremely valuable in the nineties in California: the Loma Prieta (1989) and the Northridge (1994) earthquakes had just demonstrated, once again, the inadequacy of most bridges and Caltrans (the California Department of Transportation) was launching an ambitious program to upgrade road infrastructures, and, in particular, the seven major toll bridges.

Caltrans funded the *Seismic Response Modification Device* (SRMD), an extremely powerful testing rig implemented at the University of California, San Diego [25]. This testing rig allowed controlled testing of large-scale friction pendulum systems, and in turn experimental verifications that were earlier impossible. Of the many tests performed, not all results were made public (for confidentiality reasons expressed by the manufacturer or by the user), but there is no doubt that many problems arose in the newly developed base isolators that were progressively solved [25].

This work opened the possibility to performance levels and applications otherwise very difficult, if not impossible to achieve. One example is the Benicia-Martinez bridge, retrofitted as part of the program launched by Caltrans. The bridge upgrade included all the existing bearings, which were replaced with FP devices with a nominal displacement capacity of 53 in (1346 mm), vertical load carrying capacity of 5 million pounds (about 23,000 kN) and effective period of vibration of 5 s. Each device had a diameter of about 4 m and a weight of about 18 kN [26].

With time, a number of problems and difficulties emerged, as is normal with new technology. Examples included the variability of the friction coefficient as a function of temperature and axial stress, the effects of stick-slip, and the potential for delamination. These problems will be discussed in more detail in later sections.

3.3. Influence of heating

The temperature variation in a sliding device can be approximately estimated calculating the heat flux induced by the total energy dissipated during the response to a given relative displacement history. The total dissipated energy (E_{tot}) at each sliding surface is the sum of the areas enclosed by all the force-displacement cycles. Assuming constant friction coefficient and axial force, the energy is thus the product of a constant friction force *(μN)* multiplied by the total relative displacement travelled:

$$E_{tot} = \mu N \Delta_{tot} \tag{6}$$

The temperature variation (ΔT) of a body, induced by an energy absorption (E_a), depends on its mass (M) and on its specific heat capacity (C_v, approximately equal to 500 J/kg °C in the case of steel):

$$\Delta T = \frac{E_a}{C_v M} \tag{7}$$

In regards to a double sliding surface slider, the temperature increase in the stainless steel plates and in the inner slider is not easy to estimate, for several reasons:

- The different thermal diffusivity of steel and thermoplastic pad materials, induce a major fraction of the heat flux generated to be directed towards the concave steel plate ([27]);
- The relatively low thermal conductivity of plastic materials, tends to limit the heating effects to the outer layer of the pad in sliding contact with the concave steel surface, with minor effects on the temperature of the bulk;
- The estimation of the temperature at the pad surface should thus account for (i) the thermal equilibrium between the pad and the concave surface; (ii) the generated heat flux, mainly directed towards the steel plate; (iii) the heat conduction through the steel plate; and (iv) the intermittent heat flow generated at different points of the concave steel as they enter in contact with the slider (e.g. [27–30]).

For common values of these governing parameters, local temperature variations between 15 and 30 °C per cycle can occur, with total temperature variations that can exceed 100 °C during a standard 3-cyle test at maximum displacement.

For this reason, the European Standard on Anti-seismic Devices EN 15129 [31], specifies that care is required in the execution of the test programme to ensure that any tests performed in quick succession will not excessively overheat the isolator. […] It is advisable to divide the test programme into groups of tests. After performing one group, the isolator is allowed to cool to a temperature specified by the manufacturer […] (clause 8.3.4.1.1). The tests prescribed by EN 15129 for sliding base isolators are partially reported in Table 1. It can be seen that the maximum number of complete cycles at maximum design displacement (d_{bd}) is never greater than 3.

In contrast, heating issues were not properly addressed in AASHTO [32], which prescribed each sliding bearing to be subjected to the testing protocol summarized in Table 2. Based on what discussed in this section, it is evident that a sequence of twenty cycles at the design displacement with no "cool-down" time (Test 4, Table 2) would in principle result in a temperature increase of several hundred degrees. Such a temperature increment would result in a strong variation of the apparent friction coefficient and, ultimately, by a material failure. This has been recognized and is now reflected in the 2014 edition of AASHTO ([33]), which no longer requires the performance of Test 4.

4. Development of low friction materials

4.1. PTFE, polyethylene and polyamide based materials

The devices tested and produced in California were based on a low friction material pad derived from polytetrafluoroethylene, also known as PTFE (or Teflon) from the name of a brand which uses a PTFE-derived formula. According to data available in the literature PTFE has the fundamental properties listed in Table 3.

As soon as the FP bearing patent expired, some competing companies (primarily European) started developing alternative materials,

Table 1
Partial test matrix to verify sliding isolation behavior (adapted from EN 15129).

Type of test	Displacement	Number of complete cycles
Service	Max. non seismic movement	20
Benchmark	1.0 x d_{bd}	3
Dynamic 1	0.25 x d_{bd}	3
Dynamic 2	0.5 x d_{bd}	3
Dynamic 3	1.0 x d_{bd}	3
Integrity of overlay	1.0 x d_{bd}	3
Seismic	1.0 x d_{bd}	3
Bi-directional	1.0 x d_{bd}	3
Property verification	1.0 x d_{bd}	3
Ageing	1.0 x d_{bd}	3

Table 2
Partial test matrix to verify sliding isolation behavior (adapted from AASHTO [32]).

Type of test	Displacement	Number of complete cycles
Test 1 Thermal	Max. thermal displacement	3
Test 2 Wind and Braking	Corresponding to max. wind/braking load	20
Test 3 Seismic	1.0, 0.25, 0.50, 0.75, 1.0, and 1.25 x d_{bd}	3
Test 4[a] Seismic	1.0 x d_{bd}	20
Test 5 Wind and Braking	Corresponding to max. wind/braking load	3
Test 6 Seismic Performance Verification	1.0 x d_{bd}	3
Test 7 Stability Verification	Article 15.4	1

[a] No longer prescribed in AASHTO [34].

Table 3
Low-friction material properties.

	PTFE[a]	PE[a]	UHMWPE[a]	PA[a]
Unit mass (kg/m^3)	2200	900	950	1100
Melting temperature (°C)	335	120	130–136	200–350
Unconfined compression strength (MPa)	25	12–33	38–50	55–220
Friction coefficient on polished steel (%)	5–10	15	5–10	10–20

[a] Values intended as simple references.

mainly based on formulas derived from polyethylene (PE) and polyamide (PA).

In its basic formulation, polyethylene is the common plastic and, as summarized in Table 3, has properties that are hardly compatible with the performance required to build an isolation device. However, it should be noted that more favorable features can be achieved by altering the polymer chemistry. Thus some companies have been able to produce materials that have been proven effective for base isolation applications. These materials have been validated experimentally, patented and have received *European Technical Approval* (ETA) allowing their use. The PE material currently used by European companies is referred to as UHMWPE (Ultra-High-Molecular-Weight PolyEthylene), and consists of a polymer made of long molecular chains of PE with molecular weight between 2×10^6 and 6×10^6 g/mol (note that standard linear low-density PE has a molecular weight of the order of 500 to 2000 g/mol). Increasing the length of the molecular chains entails an increase in strength, elastic modulus and wear resistance, and a decrease in ductility. Some properties of interest for UHMWPE materials are provided in Table 3.

Polyamide-based materials are more various, exist in nature and can be produced artificially. Polyamide derivatives include well-known materials such as nylon. It is again clear that materials with characteristics suitable for base isolation applications (such as those summarized in Table 3) needed to be invented, patented and validated, before an ETA could be obtained (not yet granted to any polyamide-based material).

PTFE is still used by the original producing company and it has been recently re-visited to produce effective materials by other companies [13].

While the mechanical properties of low friction materials currently in use, along with the resulting isolation devices, will be discussed in the following sections, it is evident that research and development of new materials may still provide useful results, with room for further innovation.

4.2. Typical contact pressure

Typical mean contact pressures for different low friction pad materials are in the range of 40–50 MPa for PTFE, 40–45 MPa for UHMWPE and 55–65 MPa for PA. However, these values can vary significantly, either because of different material properties or because often the contact pressure is used as a parameter to vary the apparent friction coefficient, which tends to decrease at higher pressures, as shown in Fig. 4.

Consistently with the pressure values reported, the pads are usually smaller (typical diameter between 170 and 300 mm) for PA than for PE (typical diameter between 250 and 480 mm). Smaller diameter pads may obviously imply significant cost savings, since for a given displacement capacity they result in smaller devices. However, smaller pads tend to be characterized by a larger aspect ratio and, in turn, larger internal bending moment, which results in higher stress concentration at the contact between the pad and the sliding surface.

4.3. Variation of coefficient of friction

The apparent dynamic friction coefficient varies in the range 3.0–4.5% for PA, 4.5–6.0% for PE and 6.0–8.0% for PTFE materials. However, these values need to be approached with caution for two important reasons: (i) the frictional properties of these low friction materials may vary significantly as a function of a number of parameters and two devices subjected to identical conditions, made of identical materials, may still exhibit different friction coefficients (see next section); (ii) a large variation of the friction coefficient value may be observed within the same device. For instance, the friction coefficient value may progressively decrease with the force-displacement cycles completed, as a function of the sensitivity to breakaway effects (often called "stick-slip") and to progressive heating. It should also be noted that, in this context, the friction coefficient has only been investigated at a macro-level mostly for practice-oriented calculations.

Two typical shear force-displacement loops, pertaining to PA and PE derived materials, are shown in Fig. 5. A relevant stick-slip effect is evident in the response of the PA-based device (left), while this effect is much less pronounced in the hysteresis characterizing the PE-based

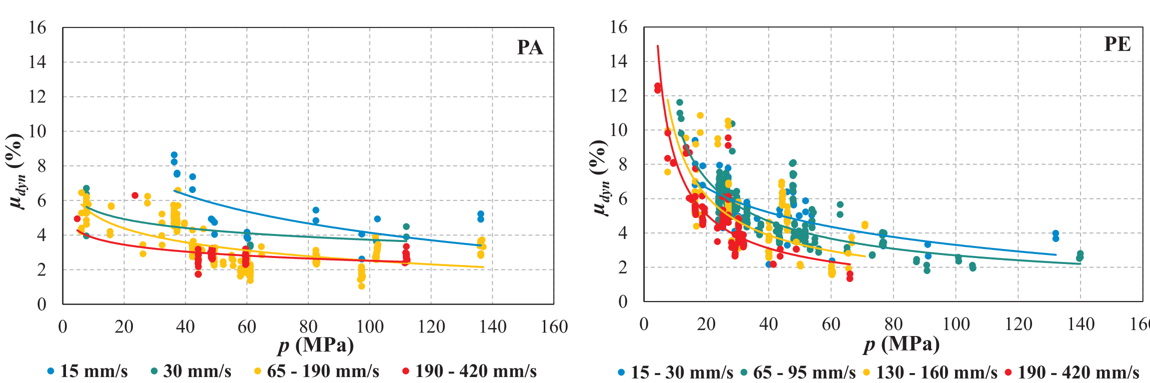

Fig. 4. Dynamic friction coefficient (μ_{dyn}) as function of contact pressure (p) and average surface velocity (v_{ave}) for devices based on PA and PE materials [13].

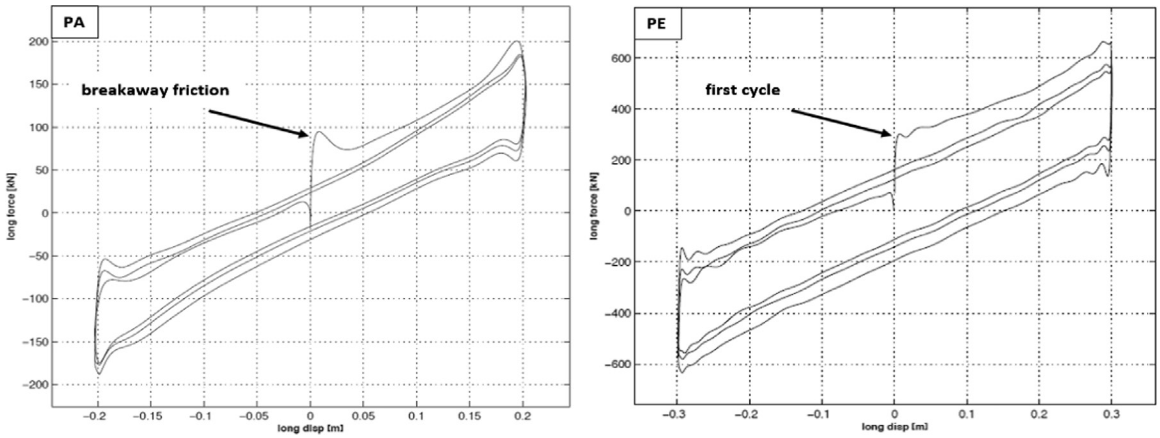

Fig. 5. Typical shear force – displacement hysteretic responses for PA and PE based FP bearings [13].

device (right). A significant reduction of the apparent friction coefficient, particularly evident with reference to the PE-based device and to the first two cycles of the response, can also be observed.

These observations are representative of a general trend: PA derived materials have been characterized by a significant stick-slip effect, at the breakaway and at load reversal, in most available experimental tests, while PE materials (likewise PTFE materials) experience hysteretic responses with only minor evidence of stick-slip effects.

Considering the expression of the equivalent damping (ξ_e), given in Eq. (2), it is evident that there is a linear correlation between ξ_e and the friction coefficient μ, if axial load, equivalent stiffness and design displacement are kept constant.

It is worth noting that the presence of stick-slip has the undesirable effect of increasing the base shear force transmitted to the isolated building and it is difficult to associate its presence to any positive phenomenon. In contrast, a higher equivalent damping increases the energy dissipation and has thus the positive effect of reducing the displacement demand.

The limitation of the base shear experienced by an isolated building is clearly one of the main purposes of adopting this solution. This results in an obvious application of capacity design principles and in the consequent protection of the building at any desired damage level, including immediate operation after a seismic event [34].

Unfortunately, the maximum shear experienced by the building does not necessarily coincide with the maximum shear transmitted at the isolation level, because of the usual presence of a foundation slab (which has a mass and an inherent dynamic response) above the isolators, and because of possible higher mode effects that may move the resultant shear force at some upper story.

The combination of these effects with stick-slip phenomena and with the variation of the effective friction coefficient between first and later cycles often results in building shear forces in the range of those predictable assuming a friction coefficient two times larger than the nominal value. This concept will be further discussed in Section 4.4.

4.4. Effects of contact pressure, velocity and temperature

As already discussed, all known low friction materials show some dependency of the apparent friction coefficient on pressure and velocity (see for example [35]). Part of this effect is certainly due to the dependency of friction on temperature, but this correlation does not entirely explain the experimental evidence.

Unfortunately, even at a global level, both pressure and relative velocity change continuously during the response to dynamic actions:

- The velocity has to approximate zero at any cycle reversal, and equals zero in all response phases with an applied shear force lower than some friction coefficient multiplied by the vertical force. From this point of view, the response to the seismic excitations consists of a number semi-cycles interrupted by extensive phases of relative rest.
- The normal force acting on each device varies continuously, as a function of vertical excitation components and/or because of overturning actions.

At a local level, i.e. at any infinitesimal point of contact, the pressure varies because of the presence of an internal bending moment due to the finite height of the inner pad (the shear forces at the upper and lower friction surfaces do not act on the same horizontal plane).

As a consequence of the uneven pressure distribution, the shear stresses are also non-uniform, since the local friction coefficient depends on pressure.

This effect may induce a rotation of the friction pad, which implies local different velocities and unpredictable relative displacement paths. Both these tendencies (spinning and wandering) have been observed experimentally.

The combination of all these effects is rather discouraging about the possibility of accurately predicting the response of an isolated system, particularly in light of the fact that micro-modeling is generally avoided because of its complexity and the associated computational costs. However, numerical studies (e.g. [23]) and experimental evidence (e.g. [36]) are consistent in indicating that using appropriate “average properties” provides acceptable approximations of the relative displacement history. It appears that most effects are compensating each other when combined to assess the global displacement history of a complex isolation system.

This evidence does not necessarily apply to the shear distribution, which may produce a global shear force resulting in potentially dangerous high local shear forces and torsional components. It seems that in-depth numerical studies based on reliable experimental evidence could still produce relevant research results in this area.

It is evident that pressure and velocity are the fundamental parameters that govern the local power generated at each sliding contact point and, consequently, the local heat flux. It is thus reasonable to try to combine all effects to evaluate the local instantaneous friction coefficient. This was attempted by [24], who considered the micro-model of a sliding device, separating the effects of velocity and temperature and calculating the temperature variation as a function of the heat flux. In the specific case considered, the friction coefficient was assumed to vary between 12% and 4% as a function of velocity, and the effect of heating on the friction coefficient was assumed to be in the range of 0.4% per degree °C. Local temperature variations in excess of 100 °C were obtained numerically and confirmed experimentally. For typical velocity ranges, the temperature appeared to be the overall dominant parameter.

5. Development of multi-surface sliders

Notwithstanding their pervasive influence on the seismic performance of buildings and bridges, traditional FP systems are affected by some limitations [37,38]. Thus, the pursuit of more efficient base isolation systems has triggered the interest of many investigators and has been the object of numerous research projects all across the world. These efforts led to the conception of a number of friction bearings that, at least pertaining to certain situations, should improve upon the performance of traditional FP bearings. Examples of such systems include Variable Frequency Pendulum Isolators [39], Multiple Sliding Bearings (e.g. [37,40–43]) and Variable Friction Systems [38,44,45,46]. Some of these systems have been taken to the point of successful validation and deployment, while others are still at a preliminary stage of development.

To this end, the two alternatives to the standard FP bearing that have been (or are being) successfully deployed and employed to protect real structures in Europe are the Double Curvature Friction Pendulum (DCFP) and the Triple Friction Pendulum (TFP) bearings. These two systems are discussed in some detail in the next subsections, along with the benefits that multiple surface sliders bring, with respect to the protection of structural and non-structural elements and the probability of collapse.

5.1. Double Concave Friction Pendulum (DCFP)

The idea of friction bearings with two sliding surfaces has been around for a long time. Some rudimentary systems were conceived and patented in the US (e.g. [9]; [47]) and in Europe [8] more than one hundred years ago.

However, it took a long time before the modern Double Curvature Friction Pendulum (DCFP) was actually developed, implemented and tested. To the knowledge of the authors, the first experience with DCFP is documented in the work of [48]. The authors presented the description and observed seismic response of a building in Japan, isolated with DCFP bearings.

The initial development of DCFP was mostly dictated by the desire of achieving base isolation devices capable of a displacement capacity two times larger than their FP counterparts. As a consequence, [48] considered devices with sliding surfaces of equal radii, equal friction coefficients and non-articulated sliders. A similar base isolation device was developed and studied, numerically and experimentally, by [49–51]. Again, the studies were limited to systems with sliding surfaces characterized by equal radii and friction coefficients. However, the device developed by [49] incorporated an articulated slider to better accommodate differential rotations and to better distribute the load on the contact surface.

[40] provided a more general description of the behavior of DCFP, accounting for the possibility of incorporating unequal radii of curvature of the two concave surfaces and/or unequal coefficients of friction of the two sliding interfaces. By making use of unequal radii and/or friction coefficients, devices with “adaptive” force-deformation behavior can be obtained (Fig. 6).

The force-displacement response of the DCFP was derived from first principles (i.e. equilibrium and compatibility), accounting for the height of the slider and the effect of friction in the rotational part of the articulated slider.

Experimental evidence was provided, along with the analytical discussion. The general behavior of a DCFP is rigid-bilinear and collapses to rigid-linear (i.e. the behavior of a standard FP bearing) for the case of equal radii and friction coefficients. In the context of numerical analyses, it was suggested that this behavior may be simulated by two single concave FP bearing models connected in series with a mass in-between representing the articulated slider. This modeling approach can be implemented in almost any available finite element software. In addition, a self-contained 3D element is now available in OpenSees [52]. Note that this 3D element was developed to simulate the response of a TFP bearing (discussed in the next section), but can be used to model a DCFP through a proper arrangement of parameters. For a more detailed discussion of DCFP systems, the reader is invited to refer to [40].

It should be noted that, while it may be possible to achieve better performing systems by using certain combinations of radii and friction coefficients, the main benefit attributed to DCFP systems over their FP counterparts is still the cost savings that can be achieved thanks to their more compact size (reducing the size of the bearing corresponds to a reduction of its cost).

Since their first development, DCFP systems have been extensively tested both numerically and experimentally (e.g. [13,18,53,54]), and have been employed as seismic protection measures in a number of projects worldwide, including in recent projects in Europe (e.g.: see Section 6.2).

An important difference between single and double surface devices is the internal bending moment induced by the applied vertical loads when the devices are in a displaced configuration. In the case of a DCFP, both structures below and above the device should be designed to be able to absorb a bending moment equal to the transmitted weight multiplied by one half of the design displacement.

In the case of a standard FP bearing, the entire displacement is applied either on the upper or lower side of the device (depending on the direction of the concave plate), resulting in a bending moment that generates only on one side of the bearing. This may be a useful feature, for example when it is important to avoid additional bending moment on a column or in the foundation.

Single surface sliders may also be effective in cases in which it is desirable to allow for a rotation (which takes place on the secondary, small radius, surface) without any significant relative displacement. This may be the case of a simply supported bridge deck, which needs to rotate to accommodate traffic loads.

Clearly, the presence of a hinge within the slider of a DCFP allows for a relative rotation, as well. However, the presence of an articulation within the slider adds a degree of freedom to the system, which may result in an apparent return to the original position of the upper and lower plate, while the slider maintains a displaced position. This situation is obviously impossible in the case of a solid slider, because of geometric compatibility. For the same reason, even with nominal identical properties at the lower and upper sliding surface, an inner hinge may favor a relative displacement at one surface only. This kind of problems are emphasized by an increased number of sliding surfaces, as discussed in the next section.

5.2. Triple Friction Pendulum bearing

The main limitation affecting standard FP systems can be associated with the impossibility of achieving optimal performance for more than one level of ground shaking [37]. Researchers have identified the answer to this challenge in devices capable of “adaptive behavior”. The expression “adaptive behavior” refers to systems whereby the stiffness, the effective friction and the damping properties change as desired, at controllable lateral displacement amplitudes. The primary benefit of this type of response is that a given isolation system can be optimized for multiple performance objectives and/or multiple levels of ground shaking. It should be noted that, in some specific situations, this behavior can be achieved through DCFP systems. However, to improve upon the DCFP, the Triple Friction Pendulum (TFP) bearing was introduced [53].

Like the DCFP, the TFP is an extension of a standard FP bearing. It consists of four spherical sliding surfaces, two sliding plates and a rigid slider, as sketched in Fig. 7 (left). The adaptive behavior of the TFP results from the different combinations of sliding that can occur on its

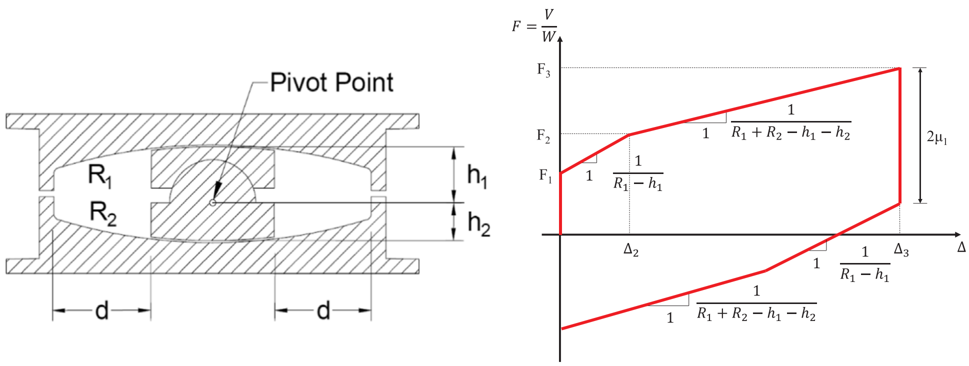

Fig. 6. View of a Double Curvature Friction Pendulum: cross-section (left); Half-cycle force-displacement relationship for DCFP bearing with $\mu_1 \le \mu_2$ (right).

multiple concave surfaces. The resulting motion occurs in up to five sliding regimes, which depend on the combination of surfaces that experience the sliding. The sequencing of the sliding regimes is a function of the coefficients of friction characterizing the various sliding surfaces and of the ratio between the surfaces' displacement capacity to their radius of curvature. The generic monotonic response of a TFP is outlined in Fig. 7 (right).

Extensive investigations on the behavior of TFP bearings, including the development of a suitable analytical model describing their cyclic response and experimental verifications, have been first conducted by [37,41,53]. Details pertaining to the construction, force-displacement relationships and relevant parameters of interest, can be found in the original publications.

In general, the results reported following these first investigations, showed a superiority of TFP bearings over FP and DCFP systems. In particular, a remarkable property attributed to the TP bearing was its effectiveness at limiting the isolator displacements in case of very rare earthquakes, while controlling drifts and accelerations for low- and moderate-level excitations.

The demonstrated capabilities of the TFP, along with the relative simplicity of this system (consisting of a passive utilizing reliable technology), further triggered the interest of the scientific community, leading to more investigations that were conducted mostly in the USA, Japan and Taiwan.

New numerical and experimental evidence (including full-scale shake-table tests, e.g. [55]) led to a better understanding of the behavior of the TFP bearing and, in turn, to the development of more refined models to describe its dynamic response. Examples include the bi-directional kinematic model developed by [56] and, most recently, the revised model proposed by [57].

Guidance for modeling TFP bearings in the context of non-linear time history analysis has also been provided. To this end, [58] described how to capture the overall force-displacement relationship of the TP bearing using three single FP bearing elements in series, which can in turn be modeled using the Bouc-Wen type plasticity model developed for the standard FP bearing [59]. As discussed for the DCFP, while this modeling approach can be implemented in almost any available finite element software, a self-contained 3D element is now available in OpenSees [52].

TFP bearings, which have been used to protect a number of structures worldwide (e.g. the Mills-Peninsula Health Services New Hospital, in California), have been successfully deployed in Europe. This is particularly true in Turkey, where they serve as seismic protective measures for a number of structures, including the Sabiha Gokcen Airport International Airport [60] and several hospital buildings (e.g. the Istanbul Okmeydanı Hospital, the İstanbul Göztepe Hospital, the Kartal Lütfi Kırdar Hospital, the Adana Heath Complex and the Elazığ hospital) ([61]).

5.3. Performance limitations of friction bearings

There is general agreement that seismic isolation can provide enhanced performance for structures under a broad range of earthquake ground motions. This improvement stems from increasing the fundamental period of vibration of the structure, and from adding a damping component to the system. Thus, base isolators contribute to reducing the earthquake-induced lateral forces transferred to the superstructure, limiting accelerations as well as displacements to the benefit of both structural and non-structural components (with some uncertainties associated with the effects of the higher modes of vibration; [62–64]). In general terms, this holds true for all kinds of base isolators, including FP bearings, DCFP and TFP bearings. The multifold benefits of base isolation have been discussed in previous sections and documented by many authors, therefore will not be discussed in much detail here. However, some considerations are provided on the effectiveness of friction bearings, with particular reference to multi-surface bearings and the achievement of multiple performance objectives.

Earthquakes can induce both horizontal and vertical accelerations. These should be discussed separately, because friction bearings provide a significantly different response in the two directions. To this end, a detailed discussion on the effects of vertical accelerations is provided in Section 7.1.

Structures isolated by means of rigid-linear bearings (such as FP bearings and DCFP with certain properties) are normally designed to achieve a certain performance, for a selected horizontal seismic demand. The bearings are therefore designed to be able to absorb a certain displacement demand under the design earthquake, ensuring that the forces and accelerations transferred to the superstructure are

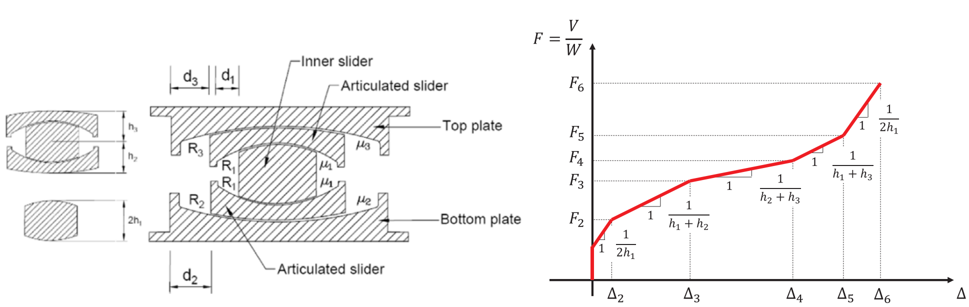

Fig. 7. View of a Triple Friction Pendulum: cross-section (left); Monotonic force-displacement response (right).

compatible with desired values. However, rare seismic events can induce horizontal demands that exceed the design values. In this case, unless the isolation system is designed with sufficient displacement capacity to absorb the larger displacements induced, giving confidence that damage (and possibly collapse) will first occur in the superstructure, the bearings will experience failure. Unfortunately, with a few notable exceptions (e.g. [54]), there have been minimal studies on the extreme behavior and collapse of friction bearings. In general, it has been shown that, to withstand very severe or near-fault motions, bearings tend to become excessively large, stiff and/or strong that they provide virtually no isolation during more frequent seismic events [65].

As discussed earlier, this challenge can possibly be overcome with multi-surface devices such as TFP bearings. TFP bearings can theoretically be designed for multiple performance objectives, as a result of the ability to achieve a multi-stage response. For example, a TFP can be designed to behave like a standard FP bearing when subjected to the design earthquake, while undergoing a somewhat stiffer response when the displacement exceeds the design value.

To this end, a number of researchers (e.g. [53,65]) reported that for moderate earthquakes, TFP bearings are comparable to conventional isolators with respect to parameters such as peak isolator displacements, while reducing drift and acceleration demands in the structure. This suggests that TFP may be more effective than traditional systems at protecting non-structural elements and contents. In addition, the outcome of these studies suggests that TFP bearings are capable of a stable performance in case of very rare events, as a result of their adaptive response.

These observations are consistent with the purpose of multi-phase bearings whose response incorporates the final stiffening stages for mainly two reasons: (i) to gradually transfer forces to the superstructure rather than impart an impact force and (ii) to delay the impact and significantly decrease the velocity when the impact occurs at the isolation level [66].

However, the results of a recent (experimental and numerical) study conducted by [66] suggest that the hardening in the response that characterizes TFP bearings may not be as beneficial as originally believed. The authors reported that the hardening phase may indeed reduce the impact forces experienced by the bearing, but only when the hardening phase is sufficiently long. Conversely, the authors observed that in some cases the hardening can actually be detrimental to the bearing failure.

While the authors acknowledge that their results require further investigations before making design decisions, the outcome of their research demonstrates that knowledge gaps associated with multi-stage friction bearings still exist.

Regardless, it is clear that the displacement capacity of the isolation system plays a key role in defining a collapse probability (assuming that the attainment of this displacement demand coincides with collapse and this, as discussed, is a coarse underestimation) while the transmitted shear governs the potential for damage and local collapse of the isolated structure.

It is interesting to note that the displacement capacity of North-American friction bearings is typically limited by the presence of a retainer ring at the boundary of the device, while this is not the case in Europe, where EN 15129 [31] does not allow the use of retainers. Thus, European friction bearings have potentially higher displacement capacity than that specified by the manufacturer because the slider has the possibility of displacing beyond the edge of the sliding surface. Although not ideal, this may be an acceptable response during a rare seismic event, provided that the slider crosses the boundary of the sliding surface by a displacement smaller than the slider's radius.

Obviously, the risk associated with the absence of a retainer ring is that, if subjected to an excessive demand, the slider could potentially lose contact and fall off the sliding surface, with catastrophic consequences. The presence of a retainer ring would prevent this from happening, but would simultaneously reduce the effective displacement capacity of the device, possibly resulting in an impact, which could result in serious problems for both the bearing and the isolated structure.

These aspects and considerations are particularly relevant with reference to ground motions that exceed the design level, and may affect the actual probability of collapse of the isolated structure.

6. Two European case studies

6.1. The Bolu Viaduct

The first relevant application of FP systems in Europe is related to the Anatolian Viaduct in Turkey [67]. The story of this long viaduct (119 spans) may be regarded as a perfect example of assessing design problems and finding ingenious solutions.

In the pre-retrofit configuration, each span consisted of fourteen “V-shaped” simply supported pre-stressed beams, resting on pot bearings with a displacement capacity of 200 mm. At each pier, a single energy dissipating unit (EDU), with a displacement capacity of 360 mm, connected the deck to the pier. The different displacement capacity of bearings and EDU's appears to be a design inconsistency [68]. In 1999, the Duzce earthquake (Nov. 12, 1999) struck the bridge. The source of the earthquake was a previously unknown fault crossing the viaduct line at an angle of approximately 15 degrees. The displacement demand resulting from the fault slip and the vibratory response of the bridge exceeded both the capacities of bearings and EDU's. As a consequence, the EDU's were destroyed (Fig. 8(a)) and the pot-bearings at most beam ends were ejected. The impact between adjacent beam ends, EDU supporting blocks and transverse shear restraint blocks occurred at most spans, destroying many of the blocks and causing extensive damage to the beam ends. Further damage occurred as a consequence of unseating from the pot-bearings, though no spans collapsed.

Large horizontal residual displacements (up to 1100 mm longitudinally and 500 mm transversely) of the beam ends were observed following the substantial fault movement and the failure of the EDU's. In a number of cases, these displacements were so large that the beam ends remained hanging over the edge of the pier cap, supported only by the link-spans through flexure and catenary action and aided by the


(a)


(b)

Fig. 8. Bolu Viaduct: (a) view of damaged EDU and loss of beam support; (b) FP bearing positioned on its support, before casting the transversal diaphragm post-tensioned beam.

fascia panels. In such cases, large vertical displacements (up to 300 mm) of the beam ends were also recorded following the earthquake. The shortening of the bridge resulting from the fault slip was largely accommodated at the movement joints, not yet installed when the earthquake struck [68].

In the aftermath of the earthquake, the local seismicity was reassessed in light of the new seismological data. This resulted in a significant increase in the intensity of the design level of ground shaking, with respect to that previously in effect. Thus, the post-event repair interventions had to be designed considering a peak ground acceleration of 0.81 g and included the following objectives:

- Repositioning deck on supports
- Lifting superstructure by 800 mm
- Constructing new transverse diaphragm beams over all supports to make superstructure continuous in 10-span segments
- Supporting the diaphragm beams on two friction pendulum bearings per support
- Replacing or repairing damaged link spans and damaged V-beam ends
- Constructing special diaphragm beams at movement joints with shear keys to restrain relative lateral movement.
- Installing seismic lock-up devices across movement joints
- Reconstructing back walls of abutments
- Installing additional piles and constructing footing overlays at six pier foundations.

The devised solution was so effective, both from a technical and an economical point of view, that truncated the pending dispute between owner and insurance company about the distinction between repair and strengthening: the insurer accepted to pay the entire foreseen cost, which was lower than what was previously expected for repair alone [67].

What is of relevance in this context, is that the final retrofit solution adopted was to replace the pot bearings and the EDU at each pier, with pairs of FP devices. The FP bearings selected had displacement capacities of 700 or 900 mm, and were placed in support of a transversal post-tensioned diaphragm beam (Fig. 8(b)).

The reference code adopted for the design and testing of the devices was AASHTO [32], which, as discussed in Section 3.3 (Table 2), prescribed the following seismic tests:

> ***Test 3, Seismic:*** *Three fully reversed cycles of loading at each of the following multiples of the total design displacement: 1.0, 0.25, 0.50, 0.75, 1.0, and 1.25, in the sequence shown.*
> ***Test 4, Seismic:*** *20 cycles of loading at 1.0 times the design displacement. The test shall be started from a displacement equal to the offset displacement.*

The initial requirement was thus to run twenty full reversed cycles at 600 mm, starting the test from an offset displacement of 300 mm (i.e.: each cycle should have run from +300 mm, to +900 mm, to −300 mm, to +300 mm). The prescribed average velocity was 0.65 m/s, which means that a total relative distance of 48 m should have been travelled in 74 s.

These requirements triggered extensive discussions, since it was evident that no friction pendulum could survive such a testing protocol, without allocating proper downtime for cooling between cycles (see Section 3.3). It is worth noting that no "reasonable" ground motion would induce a displacement demand on a base isolation device close to that imposed by the code testing protocols. At the time, this was demonstrated through a large suite of non-linear time history analyses; ultimately reasonable compromises were reached for testing. More specifically, a testing protocol consisting of four-cycle streaks, spaced out by enough time to cool down the devices was adopted.

6.2. The C.A.S.E. project

In the very first days that followed the L'Aquila earthquake of April 9, 2009, it was decided to try to avoid, or significantly reduce, the construction of temporary shelters in favor of high-tech buildings, to be used for a standard "life" duration, possibly with a modification of their use later on.

Thus, the C.A.S.E. (Complessi Antisismici Sostenibili Ecocompatibili) project was launched that involved the construction of 186 buildings, containing a total of 4449 apartments, capable of hosting approximately 15,000 people. The most critical component of the project was time. The selection of adequate locations, the assessment of those sites, the design and construction of the buildings etc. had to be performed in a matter of approximately six months.

It was immediately evident that the only way to successfully complete the project was to employ all available resources, including many different materials, construction techniques and construction technologies. In light of all this, and considering that all buildings were to be erected in high seismicity zones, it soon became clear that the most effective way to protect these structures from the effects of future earthquakes was to make use of base isolation. In addition to ensuring high seismic performance, turning to base isolation had the non-trivial benefit of drastically reducing the number and the relevance of the design variables [69].

While discussing the many challenging aspects of this unprecedented project is beyond the scope of this paper, it is of relevance to point out that, upon completion of the project, the total count of installed base isolation devices was at 7328. This extremely large number made the L'Aquila intervention the most important real life experience with base-isolated buildings.

The general properties selected for the base isolation systems were as follows:

- Displacement capacity $\Delta_d = 260$ mm
- Friction coefficient $\mu = 3\%$
- Radius of curvature $R = 4$ m
- Equivalent damping $\xi_e > 20\%$
- Vertical load capacity $W > 2820$ kN

A tolerance of ± 20% on these parameters was permitted.

Two seismic bearing manufacturers responded to the open call, demonstrating the capability of addressing all the desired specifications. One of them proposed single sliding surface devices with a polyamide-derived low friction material and ensured that all the required performance parameters would have been met. The other proposed double surface sliders, based on polyethylene materials, and ensured that all performance parameters would have been met, except for the friction coefficient which was going to be approximately equal to 4% rather than 3%. This discrepancy was deemed acceptable and agreed upon by the client.

A large number of tests were performed: 380 devices were subjected to various dynamic tests (at Eucentre), 1105 devices were tested statically, under various vertical loads, at the production sites (under the control of official public laboratories) and 15 real buildings were tested dynamically on site, using actuators installed between the isolated slab and the columns head (Fig. 9). This last kind of testing implied the excitation of a total of 600 devices (40 devices per building) and obviously included real effects such as the entire building response and the consequent redistribution of vertical load and shear force.

It is worth noting that the isolation system was designed without knowing the actual characteristics of the buildings, therefore considering wide ranges of possible weight, stiffness and period of vibration. However, the real average vertical loads on a device were between 500 and 1000 kN, i.e. in the range of 30% of the maximum vertical load considered. In addition, the velocities experienced by a base isolator responding to a seismic event may vary significantly. For instance, a

Fig. 9. In situ testing of an isolated building in L'Aquila.

bearing with an effective period of vibration T = 4 s, performing full cycles at peak displacement ± 260 mm, has an average velocity of 260 mm/s, and a theoretical maximum velocity of 408 mm/s. However, in reality, the period of vibration varies continuously and each displacement cycle depends on the characteristics of the ground motion.

Thus, different velocities and axial force levels were adopted during the experiments, to account for all possible scenarios. The variability of the results as a function of contact pressure and velocity was somewhat surprising, showing the following main features:

a) The breakaway friction was in the range 10–15%.
b) The low-velocity friction coefficient (i.e. velocity lower than 50 mm/s) was around 5–6% for polyamide and 8–9% for polyethylene, with vertical force around 2000 kN, and increased to 8–12% and 14–19%, respectively, with vertical force around 500 kN.
c) The high-velocity friction coefficient showed relatively low variations (± 10–20% with respect to the average value) when the velocity varied between 100 and 300 mm/s, but appeared to be sensitive to the applied vertical load, with values around 3% at 2000 kN and 4.5% at 500 kN for polyamide and around 5–6% at 3000 kN raising to 8–10% at 1000 kN and even close to 15% at 500 kN for polyethylene.
d) The equivalent damping values estimated for the actual range of possible loads and velocities were in the range of 15–25% for polyamide, but significantly higher than prescribed for polyethylene, with values between 25% and 45%.

Graphs showing approximate values of the friction coefficient as a function of vertical load and velocity, are depicted in Fig. 10. As discussed, the polyethylene based devices are generally characterized by a higher friction coefficient (and consequently a higher damping) and a smoother variation of friction with velocity and contact pressure. Polyamide based devices experience a much higher variation of the apparent friction at low contact pressure and low velocity, typical of stick-slip like phenomena.

From this data, it became fundamental to evaluate the effects of these unexpected/undesirable phenomena on the expected damage, and eventually on the probability of collapse, of both the base isolation systems and the buildings.

Thus more refined analyses of the base-isolated buildings were conducted, incorporating in the numerical models aspects that had been neglected during the preliminary design phases. All buildings were modeled according to their real characteristics, considering their mass, stiffness and local soil conditions, and their response was re-assessed via non-linear time history analysis. The input for the analyses consisted of suites of sixteen couples of spectrum-compatible ground motion excitations.

A comprehensive parametric framework was built, to ensure that all possible combinations of parameters were addressed. The relevant variables included:

- Structural materials: concrete, steel and timber;
- Lateral load resisting systems: moments resisting frames and shear walls;
- Mass: the heaviest to lightest building mass ratio was equal to 3;
- Soil conditions.

The results of the analyses indicated that the displacement demand on the isolators was always substantially lower than the design displacement (i.e. 260 mm), with maximum values in the range of 190 mm.

Despite the much higher than expected friction coefficients (both static and dynamic) characterizing the isolation devices, the analyses showed that the building strengths were adequate. The majority of the recorded building capacity-to-demand ratios varied between 1.0 and 1.6, but the highest value was equal to 2.3. However, this outcome was partly attributed to the real strength of the buildings, generally higher than the prescribed minimum design value. The resulting inter-story drifts varied as well, generally between 0.1% and 0.2%, with peak values never higher than 0.4%. Typical values of the base shear were strongly dependent on the period of vibration of the buildings, with values between 10% and 25% of the building weight for periods ranging between 0.1 and 0.3 s.

The in-situ tests discussed earlier, provided results essentially in line with the numerical outcome. The testing system allowed the application of one half cycle, at maximum displacement and velocity of about 250 mm/s (the design velocity).

The results of the tests indicated a very uniform range of periods of vibration of the buildings, with an average period of 0.21 s (with a standard deviation σ = 0.05 s) considering the response in both directions. Since the masses of the buildings varied by factors up to 3, it was evident that buildings with higher mass were characterized by

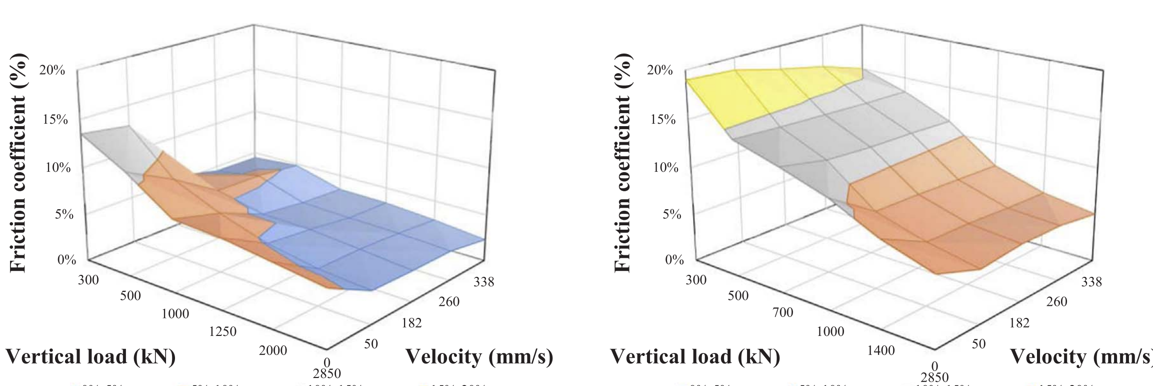

Fig. 10. Variability of the friction coefficient, as a function of vertical load and velocity, for the devices used in the aftermath of the L'Aquila earthquake (left: polyamide material; right polyethylene material).

higher stiffness. The recorded acceleration at the base slab never exceeded 0.09 g, while the maximum accelerations recorded at the building floors were approximately equal to 0.16 g.

While these results had no practical consequences for the project, they did raise a number of interesting points:

- The dependency of friction on contact pressure and velocity should be further investigated, and possibly reduced, developing new materials. In this framework, the effects related to temperature change should be considered and fully understood.
- Proper values of the friction coefficient should be used in the global response verification, considering appropriate ranges of variation of contact pressure and velocity, along with stick-slip effects.
- Upper and lower bound values should be always adopted for the friction coefficient, to estimate the maximum displacement demand, but particularly the building shear and inter-story drift demands.
- Refined numerical models of each device, including the local variation of friction at the different locations of the sliding interface, the internal bending and torsional moments and rotation, may provide more insights into the real global response.
- Tests on materials and qualification and acceptance tests on isolation devices should be performed considering the extensive variation of contact pressure and velocity, to characterize the entire potential response.

Most of these considerations do not appear to have been fully adopted, in research and in practice, some seven years later.

7. Open problems and current developments

7.1. Response to vertical actions

Vertical actions may arise in structures during seismic events, as a result of the overturning effects resulting from the earthquake-induced lateral forces and because of vertical acceleration components characterizing the earthquake ground motion.

The importance of vertical actions with respect to the response of friction base-isolated structures has been investigated, directly and indirectly, by various authors (e.g. [11,23,70–75]). While somewhat conflicting outcomes emerge from the data available in the literature, the general trend can be summarized as follows: while sliding base isolators are excellent means of protecting buildings from the effects of the horizontal components of a ground motion, the presence of vertical actions can compromise functionality, reducing their efficacy and jeopardizing their performance.

To this end, vertical actions from overturning effects and those induced by the presence of vertical components of excitation are in some ways distinct phenomena, and need to be discussed separately.

Overturning effects are normally a concern in slender structures with large height-to-width aspect ratios and in buildings incorporating bearings below braced columns or stiff walls [76], as well as in certain types of bridges with large ratios of height of the center of mass to the distance between the bearings [23]. In structures with these characteristics, the overturning induced by the lateral forces may be significant, resulting in substantial vertical contact pressure variations (illustrated in Fig. 11) and, in some extreme cases, in the uplift of the bearings.

It was discussed earlier in this paper, how the response of friction base isolators, such as FP bearings, is strongly dependent upon the vertical load acting on the bearing and the friction coefficient characterizing the contact between the pad and the sliding surface. FP bearings behave essentially rigidly as long as the acting shear force is smaller than the vertical load on the bearing, multiplied by the static friction coefficient. Upon activation, the shear strength of the device increases proportionally to the experienced lateral displacement and to the ratio between the acting vertical load and the radius of curvature of the sliding surface.

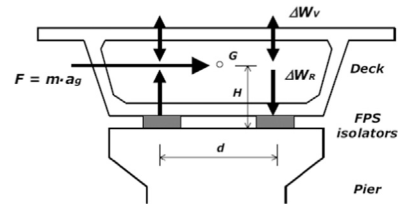

Fig. 11. Overturning-induced axial force variations in bridge bearings (adapted from [23]).

In this context, overturning actions, which can either increase or decrease the initial vertical load on a bearing, inevitably influence the bearing behavior. Most notably, varying the vertical load (and in turn the vertical contact pressure), may significantly affect the bearing activation force, its post-activation stiffness and the frictional properties of the device.

To this end, experimental results pertaining to more than 1000 tests performed on friction bearings including single and double FP bearings, showed that lower vertical loads (i.e. lower contact pressures) result in higher and more “unstable” friction coefficients. In contrast, higher vertical loads (i.e. higher contact pressures) tend to produce consistently lower friction coefficient values [13]. This was shown in Figs. 4 and 10, where the observable trends outlined that stable friction coefficients are only obtained once the contact pressure on the bearings is higher than approximately 50 MPa.

All this may turn into a series of undesirable effects, such as (but not limited to):

- Bearings working in parallel subjected to different vertical loads experience different behavior, resulting in a non-uniform and perhaps less controllable response of the base-isolated system
- Because of the high variability of the friction coefficient value at low contact pressures, lightly loaded bearings subjected to identical vertical loads, may have consequences analogous to those addressed at the previous point
- Bearings subjected to significantly higher vertical loads tend to provide higher lateral resistance than others. This may result in stress concentrations and local damage. Also, some or the protected structural elements may experience important demand increments and torsional effects may arise
- Bearings subjected to excessive vertical contact pressures (i.e. much higher than the design values) may experience malfunctioning or failure
- There may be a loss of contact between the pads and the sliding surface (i.e. uplift) in bearings subjected to excessive “tensile” vertical loads. This may have a series of implications that will be discussed in more detail in the next section.

Issues associated with the vertical acceleration components of an earthquake are normally more relevant in near-field, but may be present in other types of events. Although often deemed secondary, vertical excitation components can be characterized by very high PGA values and be the cause of extensive damage to the built environment. For instance, recorded vertical PGA reached up to 2.2 g during the Mw 6.2 Christchurch earthquake of 2011 [77].

Evidence emerged from some of the available experimental studies on reduced scale structures, base-isolated with single and multi-spherical friction bearings, seems to suggest that vertical excitation has minor influence on the horizontal response and performance of friction bearings (e.g. [65,72]). However, this is in contrast with the results of recent test programs performed on full-scale isolated buildings conducted at the E-Defense shaking table of Japan [74,75,78]. More specifically, one of the main outcomes of these studies was the significant influence of vertical excitation on the overall performance, and the amplification of the horizontal accelerations recorded at the various levels of the building as a consequence of the multi-directional excitation.

Vertical accelerations were observed to be particularly detrimental for non-structural elements which did not appear to benefit significantly from the presence of the base isolation system. Furthermore, the outcome of the experimental programs suggested that the vertical motion transmitted to the various levels of the building and to non-structural components and content, is relatively insensitive to the base conditions. This means that friction base-isolated structures and fixed-base systems have analogous response to vertical excitations.

This outcome is consistent with conclusions emerged from the analysis of the vertical accelerations recorded at various levels of base-isolated buildings during real seismic events, such as the 1994 Northridge earthquake. For instance, after examining several instrumented buildings, [78] concluded that vertical accelerations transmitted from the ground to the higher floors were not affected by the presence of the isolation system, and that the structures behaved essentially as fixed-base systems.

These results can be attributed to the high vertical stiffness that characterizes friction bearings, which produces a vertical isolation period of vibration around 0.03 s [7]. It is evident that systems with these characteristics provide only horizontal isolation, while behaving as fixed with respect to vertical excitations.

7.2. Uplift

Traditional friction bearings provide no resistance to tensile forces and are consequently free to uplift. Bearing uplift may occur under certain conditions which include the presence of high vertical accelerations and/or substantial overturning. This may produce detrimental effects to the isolators or to the protected structure performance, which may be in the form of bearing damage due to excessively large compressive forces arising upon re-engagement or demand amplifications on the structural members, amongst many others.

To the knowledge of the authors, friction isolator failures that were clearly due to bearing uplift during real earthquakes have not been documented. Although not extensively, uplift issues have been investigated and observed experimentally, via shake-table tests, in the US and in Japan.

For instance, uplift of multi-surface pendulum bearings was observed experimentally by [50], during an extreme tri-directional shake-table test. In this test, the authors recorded a peak uplift of 17 mm, at which point there was a clearly visible separation between the top concave plate and the slider. Interestingly, the isolation system did not show any sign of distress upon returning from uplift, behaving as expected for the remainder of the test program, without the need of any repairs.

Analogous conclusions were drawn by [73], who observed short duration (< 0.25 s) uplift of Triple Pendulum bearings during a series of harmonic tests conducted on slender building specimens. Consistent with the findings of [72,73] reported that the cyclic behavior of a Triple Pendulum bearing does not seem to degrade or vary significantly following the uplift. In fact, the slider assembly appeared stable and the bearing hysteresis was not affected other than a localized reduction in horizontal shear due to the interaction of shear and supported axial load through friction.

Simultaneous uplift of 9 Triple Pendulum bearings was observed by [75], while testing a full-scale base-isolated five-story, steel moment-frame building, on the E-Defense shake-table. The bearing uplift and the consequent bouncing of the entire building on the shake-table, was induced by a large vertical acceleration pulse with PGA = 1.3 g. The main consequence of this intense vertical shaking was a series of high-frequency acceleration spikes that significantly amplified the table acceleration in the columns at all floors (up to a factor of 7 in the top-story columns). However, this high-frequency shock was not transmitted to the slabs, and it did not appear to induce damage to the structural elements or the building content. The vertical accelerations and the resulting bearing uplift were adequately absorbed by the structure and the isolation system, without notable consequences.

Overall, the experimental evidence collected thus far seems to suggest that uplift of friction bearings during an earthquake may not represent a significant issue. However, such a statement should be made with caution, on account of the very limited information available on the matter. In particular, the uplift behavior documented in the literature had very short durations (i.e. fractions of a second), and small separation distances. In addition, the uplift was essentially vertical, with the bearings undergoing no lateral motions while the parts were not in contact. Under these specific circumstances, bearing uplift seems to have no adverse effect on the general performance of the bearing.

Nevertheless, under more extreme circumstances, bearing uplift could have more serious consequences. For instance, uplift occurrence could be catastrophic, in case the separation distance exceeded the height of the retainer ring (if present), and/or in situations where the top and bottom part of the bearings lost contact while in relative lateral motion [72]. Even though this and other behaviors have never been observed, and seismically-isolated structures are currently designed so that uplift in sliding bearings is largely avoided (e.g. verifying via non-linear time history analysis that no bearings experience tensile loads during a design level multi-directional seismic event, or by means of bearings with tensile retention capacity, as discussed in the next section), the possibility of serious uplift issues should be investigated as part of future studies.

7.3. Tensile retention capacity

In response to the issues discussed in the previous sections, several authors have explored the possibility of developing base isolator devices equipped with some tensile retention capacity, and a number of uplift-restraint mechanisms have been proposed.

A brief review of uplift-prevention systems implemented or proposed for use with sliding bearings is provided in this section. For a more thorough discussion on the topic, the reader can refer to the work of [79].

The first uplift-restraint mechanism that could be theoretically implemented in parallel with different kinds of sliding bearings, was developed by [80] in Japan. This system consists of two orthogonal steel arms connected to the superstructure slab and to the foundation of the structure, respectively. These arms, normally not in contact with each other, interlock in case the structure undergoes uplift in excess of a predefined tolerance. Even though the impact of this mechanism on the behavior of the isolation-system has not been investigated in detail [79], this technology has been used on the Excel Minami-Koshigaya 10-story building in Koshigaya City.

[81] conducted an experimental study to evaluate the feasibility of using a sliding isolation system with uplift-restraint devices for medium-rise buildings subject to column uplift. The isolation system consisted of flat sliding Teflon bearings acting in parallel to a series of helical spring units, intended to provide re-centering forces [82]. The uplift-restraint mechanism was provided by L-shaped steel profiles, bolted to the top part and extending under the bottom part of the slider on two sides, as shown in Fig. 12(a).

The results of the shake-table tests and the numerical analyses performed, demonstrated the effectiveness of this system in resisting tensile forces, preventing bearing uplift. This concept was subsequently extended to sliding bearings with a curved surface, and was employed as a seismic protective measure in real structures (e.g. San Francisco approach to the Oakland Bay Bridge, Fig. 12(b)).

However, this approach was conceived, implemented and validated only for unidirectional excitation. Extension to multidirectional scenarios is difficult and thus the field of application of this mechanism is somewhat limited.

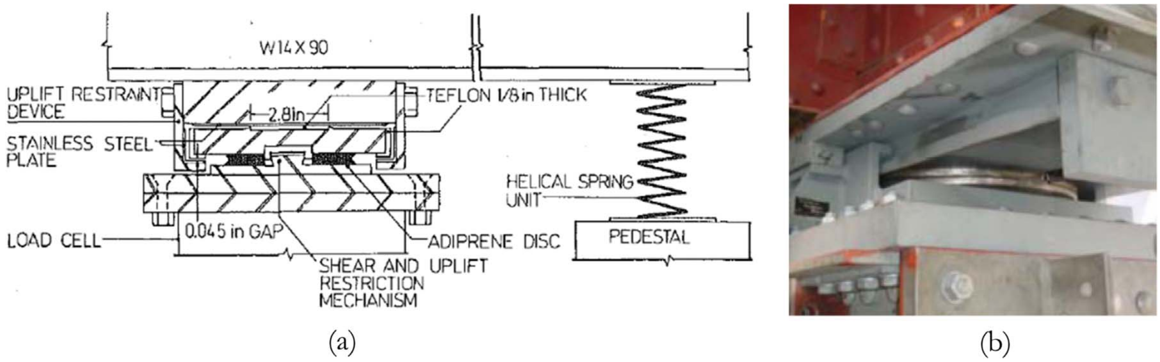

Fig. 12. (a) Section of Teflon Disc Bearing with uplift-restraint devices, and helical spring unit (adapted from [81]); (b) view of unidirectional FP bearing with uplift-restraint installed at the San Francisco approach to the Oakland Bay Bridge (adapted from [79]).

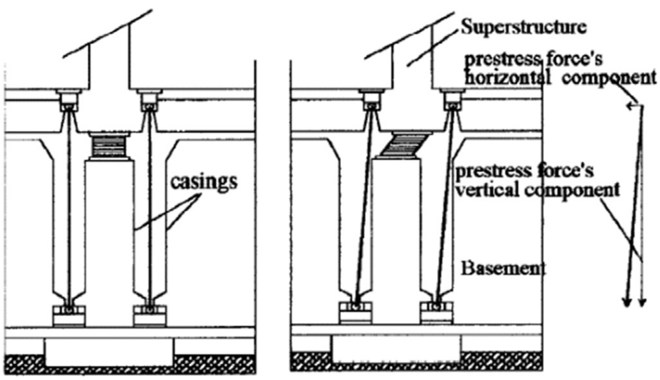

Fig. 13. Prestressed elastomeric bearings in undeformed and deformed configuration (adapted from [83]).

[83] proposed to solve bearing uplift issues by combining common seismic isolation bearings with pairs of vertical prestressed tendons, located on the sides of the bearing (Fig. 13). This technique was initially proposed for use with elastomeric bearings, but it can be theoretically paired with all kinds of isolation systems, including sliding bearings, being external to the mechanism of the isolation system.

The idea behind "prestressed earthquake isolators" is quite simple: the prestressed cables are used to provide sufficient additional compressive force on the bearings, preventing the development of tensile forces or uplift. However, while theoretically effective and predictable in behavior, this system has complex practical implications and, in some instances, may impact the performance of the isolation system [79].

More recently, [76] introduced an innovative uplift-restraint sliding bearing, referred to as *XY*-FP. Conceptually, and in absence of vertical excitations, this system works as a traditional FP bearing. However, unlike an FP bearing, the XY-FP is made of two separate orthogonal concave sliding rails, interconnected through a mechanism that can slide along both rails (Fig. 14). Thanks to this arrangement, this isolator is capable of an uncoupled bi-directional response, while permitting tensile forces to develop in the bearing thus preventing uplift.

The effectiveness of this system has been demonstrated, both experimentally and numerically, by [76,79,84]. As a result, the *XY*-FP has been used in real-world applications and has been successfully implemented in a number of occasions. Examples include the Los Angeles Emergency Operations Center (LA EOC) in California and the Linked Hybrid Complex in Beijing in China [79].

7.4. Residual displacement

In modern performance-based design and assessment frameworks, the post-earthquake residual displacement is recognized as one of the key structural response parameters. Thus, an effective base isolation system should be equipped with some restoring capability to be able to re-establish its initial configuration following a seismic event.

Permanent offsets in the base isolation system are undesirable for a number of reasons: first, deformed base isolators can absorb lower displacement demands and may not be able to withstand aftershocks and, more generally, future events; second, excessive residual displacements may affect the serviceability of the structure and possibly jeopardize the functionality of elements (e.g. fire protection elements, joints of primary piping systems etc.) crossing the isolation plane. Clearly, base-isolated structures should be designed and detailed to accommodate expected permanent offsets.

Understanding and being able to control the residual displacement of base isolation systems is particularly important for structures located near faults, where it is common to record pulselike ground motions [85]. It has been shown that near-fault earthquakes can induce significant residual displacements in isolation systems with inadequate restoring capability [86,87].

Residual displacement considerations are also critical for flat sliding bearings, which do not have any restoring capacity and can tend to "migrate" over an increasingly large distance the longer an excitation

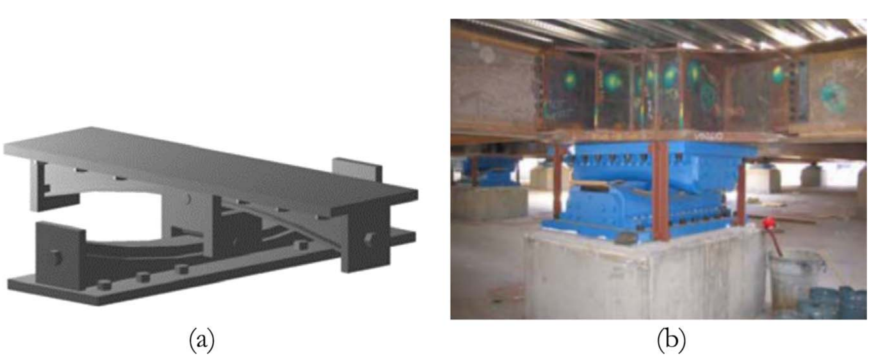

Fig. 14. (a) Three-dimensional view of the uplift-restraining *XY*-FP isolator (adapted from [79]); (b) Installation of *XY*-FP tension-capable bearings in LA EOC in California (adapted from [79]).

lasts (or the more excitations they are hit by). This is indeed evident with reference to a flat Coulomb slider, where the behavior is identical at every point within its range with no preference to return to its starting position. In this way, the displacements of a flat slider can be equated to that of a random walk, or Brownian motion, for which the expected displacement increases monotonically as a function of time.

While there are no clear indications as to how the post-event residual displacement in a base isolation system should be estimated, modern seismic codes incorporate recommendations aimed at ensuring that a selected isolation device possesses adequate restoring capability.

For instance, for sliding bearings, the 2001 California Building Code [88], the 1999 AASHTO Guide Specifications for Seismic Isolation Design [32] and the International Building Code [89], attempt to achieve adequate "self-centering" base isolation systems by introducing limits on the minimum post-activation (or post-sliding) stiffness (K_p) that a system should possess, and/or by limiting the effective period of vibration of the system, calculated proportionally to the post-activation stiffness of the bearing (i.e.: $Te = 2\pi\sqrt{M/K_p}$, M is the mass of the structure), below pre-determined values.

At the same time, the IBC 2006 requires that the restoring capability requirement may not be deemed fulfilled if the isolation system does not remain stable under full vertical load and horizontal displacements up to 3.0 times the design displacement.

On the other hand, the Eurocode 8, EN1998-2 for seismically isolated bridges [22] imposes limits that involve both the lateral force and the lateral displacement of the isolation system, effectively dictating more stringent limits on its hysteretic behavior.

It should be noted that, although current code recommendations on residual displacement in base isolation systems represent a good starting point, they are not necessarily based on solid theoretical fundamentals, but rather on experience and on limited experimental evidence [19]. Furthermore, a thorough examination of the literature available on this topic indicates that the restoring capability of friction bearings has received little attention, and still represents a major research gap [19].

Examples of available experimental studies on the residual displacement of friction bearings include those by [18,24,72]. The main outcome of these experimental campaigns is that friction devices with maximum displacement to "static residual displacement" ratio (d_{max}/d_{rm}) greater than 0.5, possess good restoring capability.

This finding is consistent with the results of numerical investigations conducted by a number of authors (e.g. [19,86,90,91]). In particular, the results of some of the available numerical studies on base isolation systems (e.g. [86]) showed that the main parameter that affects the restoring capability of bilinear isolation systems is indeed the ratio between the absolute value of the peak displacement (d_{max}) and the maximum static residual displacement (d_{rm}, the residual displacement where static equilibrium is reached when the system is unloaded under quasi-static condition from its peak displacement). Both these parameters depend on the shape of the hysteretic behavior of the isolation system. In addition, it was demonstrated that the restoring capability of isolation systems strongly depends on the earthquake characteristics. However, the statistical analyses carried out thus far seem to confirm that bilinear isolation systems with $d_{max}/d_{rm} > 0.5$ exhibit negligible residual displacements.

However, there are at least two important aspects related to residual displacements in base isolation systems still to be addressed that can be summarized as follows:

1. What should the hysteretic response of an "optimal" base isolation device look like?
2. How can the maximum residual displacement of a base isolator be accurately estimated, as a function of the seismic demand and the design parameters?

There is no simple answer to either of these questions. In addressing the first question, one should keep in mind that the two key properties of a base isolation system, namely energy dissipation and self-centering capability, are two antithetic functions. Increasing self-centering properties inevitably reduces energy absorption capabilities and vice-versa. Therefore, achieving the best performance with respect to one parameter of interest (e.g. negligible residual displacement) may result in an unacceptable overall performance of the system (e.g. too high lateral forces and/or accelerations attracted by the system). Furthermore, a number of practical constraints may come into play. For instance, to obtain negligible residual displacement in a sliding system, it is preferable to manufacture devices with small radius of curvature. However, the use of a small radius of curvature may result in unacceptable vertical fluctuations of the isolated structure that can only be reduced introducing systems with a larger radius of curvature (which, in turn, would result in larger residual displacement).

Addressing the second question is, to some extent, more important and represents the real research priority. Being able to control the residual displacement of an arbitrary sliding base isolator would allow designers to converge to desired solutions, with full control on the outcome. The attention could be finally shifted from trying to minimize (or eliminate) residual displacement in base isolators at all costs, to consciously designing for a residual displacement value that is deemed acceptable, implementing all the necessary construction details to accommodate and efficiently absorb the expected post-event offsets.

8. Conclusions

This review paper has presented an overview on the state of the art of friction-based isolators, with a focus on systems that have found their way into European applications. In going through the evolution and development of these systems, the most notable contributions originated in the US and worldwide were also included.

It is evident that a number of isolation systems are at a stage that they can be used to effectively protect buildings and other structures from the effects of strong earthquakes. For instance, systems such as FP bearings and DCFP have found relatively broad applications both in Europe and worldwide. TFP systems have also been used in a number of international projects. However, it is also evident that a number of aspects characterizing the behavior of friction-based isolators need to be further investigated, better understood, and possibly improved.

Although extensive research has been conducted to reduce undesirable stick-slip phenomena and to determine the relations between parameters such as friction coefficient, velocity and vertical contact pressure, uncertainties still exist. In this context, experimental verifications of the device properties play a fundamental role. Thus, it is important to clearly define reliable testing protocols to be adopted.

Impressive progress has been made on the side of numerical modeling and analysis of base isolators and base-isolated structures. Three-dimensional models capable of accounting for complex aspects of the base isolators' behavior, such as the dependency of friction on contact pressure and velocity, are now available and can be used in the context of non-linear time history analyses. It is not clear if more refined models, capable for example of accounting for "local" effects, such as spinning and wandering, are required or if simpler "macro-models" are sufficiently accurate.

The response of friction bearings to vertical actions represents an important area of research. Friction bearings are not meant to offer protection against vertical accelerations which may in fact negatively affect their performance (by altering the vertical contact pressure and, in turn, the device behavior) and, in some extreme cases, experience uplift and ultimately failure. Furthermore, vertical ground acceleration components are rarely considered while conducting the analysis of base-isolated structures and there is an evident lack of guidance on this topic. Recent experimental evidence has emphasized the importance of incorporating these aspects in the analysis, as vertical actions may be detrimental to the performance of the base isolation system but also to that of structural and non-structural elements.

Current design methods available for base isolation systems (e.g. Displacement Based Design procedures) generally provide accurate predictions of the response of base-isolated structures, particularly in regards to the expected peak displacements. However, numerical studies have demonstrated that the prediction of the base shear, as well as of the lateral forces and accelerations along the height of a building, are often less reliable. This has been often attributed to the effects of the higher modes of vibration and to some of the modeling assumptions adopted to conduct the numerical analyses (e.g. the viscous damping model assigned to the structure). In any case, this remains an open problem that needs to be properly addressed. In particular, in a design context, it is necessary to define appropriate protection factors and acceptable ductility demand and inter-story drift levels. Improved approaches to estimate expected residual displacements, along with criteria to evaluate their relevance with respect to the achievement of a desired performance, should also be developed.

Most recently, researchers have been working on responding to the need of developing base isolation devices capable of achieving multiple performance objectives, at different levels of earthquake intensities. This led to the development of multi-surface devices, such as DCFP and TP, which are capable of adaptive behavior and can be potentially optimized for different earthquake magnitudes. However, a number of questions remain and the development of systems capable of adaptive behavior, and more generally of better performing devices, remains one of the research priorities and is currently the object of several ongoing research projects.

References

[1] Kelly JM. Aseismic base isolation: review and bibliography. Soil Dyn Earthq Eng 1986;5:202–16.
[2] Buckle IB, Mayes RM. Seismic isolation: history, application, and performance – a world view. Earthq Spectra 1990;6:161–201.
[3] Taylor AW, Lin AN, Martin JW. Performance of elastomers in isolation bearings: a literature review. Earthq Spectra 1992;8:279–303.
[4] Soong TT, Constantinou MC. Passive and active structural vibration control in civil engineering. New York, NY, USA: Springer-Verlag; 1994. p. 1994.
[5] Kunde MC, Jangid RS. Seismic behavior of isolated bridges: a-state-of-the-art review. Electron J Struct Eng 2003;3:140–70.
[6] Symans MD, Cofer WF, Fridley KJ. Base isolation and supplemental damping systems for seismic protection of wood structures: literature review. Earthq Spectra 2003;18:549–72.
[7] Warn GP, Ryan KL. A review of seismic isolation for buildings: historical development and research needs. Buildings 2012;2:300–25.
[8] Barucci C. La casa antisismica [The antiseismic house]. Gangemi, Rome (In Italian); 1990.
[9] Touaillon J. Improvement in buildings. US patent 99973; Feb. 15, 1870.
[10] Kelly JM, Chalhoub MS. Earthquake simulator testing of a combined sliding bearing and rubber bearing isolation system Berkeley, CA, USA: University of California; 1990. (Report No. UCB/EERC-87/04).
[11] Zayas V, Low S, Mahin S. The FPS earthquake resistant system. Experimental report UC Berkeley; 1987. (Report No. UCB/EERC-87/01).
[12] Danusso A. Le costruzioni antisismiche (The seismic resistant constructions, in Italian). Il monitore Tecnico, (journal on engineering, architecture, mechanics, electronics, railways, agronomy, cadastre and industrial arts – official body of the association of former students of the Politecnico di Milano); 10 August 1909.
[13] Barone S, Calvi GM, Pavese A. Experimental dynamic response of spherical friction-based isolation devices. J Earthq Eng 2017. http://dx.doi.org/10.1080/13632469.2017.1387201.
[14] Zayas V. Earthquake protective column support. US patent 4644714; Feb. 24, 1987.
[15] Zayas VA, Low S, Mahin S. A simple pendulum technique for achieving seismic isolation. Earthq Spectra 1990;6(2):317–33.
[16] Priestley MJN, Calvi GM, Kowalsky MJ. Displacement based seismic design of structures. Pavia: IUSS Press; 2007.
[17] Cardone D, Gesualdi G. Influence of residual displacements on the design displacement of spherical friction-based isolation systems. Soil Dyn Earthq Eng 2017;100:492–503.
[18] Ponzo FC, Di Cesare A, Leccese G, Nigro D. Shake table testing on restoring capability of double concave friction pendulum seismic isolation systems. Earthq Eng Struct Dyn 2017. http://dx.doi.org/10.1002/eqe.2907.
[19] Cardone D, Gesualdi G, Brancato P. Restoring capability of friction pendulum seismic isolation systems. Bull Earthq Eng 2015;13(8):2449–80.
[20] Quaglini V, Gandelli E, Dubini P. Experimental investigation of the re-centring capability of curved surface sliders. Struct Control Health Monit 2017;24(2):e1870.
[21] Quaglini V, Gandelli E, Dubini P, Limongelli MP. Total displacement of curved sur sliders under nonseismic and seismic actions: a parametric study. Struct Control Health Monit 2017. http://dx.doi.org/10.1002/stc.2031.
[22] CEN. Eurocode 8: design of structures for earthquake resistance – Part 2: bridges. EN1998-2. Bruxelles, Belgium: European Committee for Standardization; 2005.
[23] Calvi GM, Ceresa P, Bolognini D, Casarotti C, Auricchio F. Effects of axial force variation in the seismic response of bridges isolated with friction pendulum systems. J Earthq Eng 2004;8(S1):187–224.
[24] Quaglini V, Gandelli E, Dubini P, Vazzana G, Farina G. Re-centring capability of friction pendulum system: experimental investigation. In: Proceedings of the 2nd European conference on earthquake engineering and seismology. Istanbul, TK; 2014.
[25] Shorthreed JS, Seible F, Benzoni G. Simulation issues with a real-time full-scale seismic testing system. J Earthq Eng 2002;6(S1):185–201.
[26] Zayas VA, Low S, Mokha AS, Imbsen RA. Seismic isolation of Benicia-Martinez bridge. In: Proceedings of ASCE structures congress; 2001. (published on line. 〈http://dx.doi.org/10.1061/40558(2001)121〉).
[27] Quaglini V, Bocciarelli M, Gandelli E, Dubini P. Numerical assessment of frictional heating in sliding bearings for seismic isolation. J Earthq Eng 2014;18:1198–216.
[28] Constantinou MC, Whittaker AS, Kalpakidis Y, Fenz DM, Warn GP. Performance of seismic isolation hardware under service and seismic loading. Report MCEER-07-0012. Multidisciplinary Center for Earthquake Engineering Research, State University of New York at Buffalo; 2007.
[29] Kumar M, Whittaker AS, Constantinou MC. Characterizing friction in sliding isolation bearings. Earthq Eng Struct Dyn 2015;44:1409–25.
[30] Lomiento G, Bonessio N, Benzoni G. Friction model for sliding bearings under seismic excitation. J Earthq Eng 2013;17:1162–91.
[31] European Standard EN 15129:2010 for anti-seismic devices, European Committee for Standardization; November 2010.
[32] AASHTO. Guide specifications for seismic isolation design. 4th ed. Washington DC: American Association State and Highway Transportation Officials; 1999.
[33] AASHTO. Guide specifications for seismic isolation design. 2nd ed. Washington DC: American Association State and Highway Transportation Officials; 2014.
[34] Christopoulos C, Filiatrault A. Principles of passive supplemental damping and seismic isolation. IUSS Press, Istituto Universitario di Studi Superiori di Pavia; 2006.
[35] Mokha A, Constantinou MC, Reinhorn AM. Teflon bearings in base isolation I: testing. J Struct Eng (ASCE) 1990;116:438–544.
[36] Al-Hussaini TM, Zayas VA, Constantinou MC. Seismic isolation of multi-story frame structures using spherical sliding isolation systems Buffalo, NY: University at Buffalo; 1994. (Report No. NCEER-94-0007).
[37] Fenz DM, Constantinou MC. Spherical sliding isolation bearings with adaptive behavior: theory. Earthq Eng Struct Dyn 2008;37(2):163–83.
[38] Calvi PM, Ruggiero DM. Numerical modelling of variable friction sliding base isolators. Bull Earthq Eng 2016;14(2):549–68.
[39] Murnal P, Sinha R. Earthquake resistant design of structures using the variable frequency pendulum isolator. J Struct Eng 2002;128(7):870–80.
[40] Fenz DM, Constantinou MC. Behaviour of the double concave Friction Pendulum bearing. Earthq Eng Struct Dyn 2006;35:1403–24.
[41] Fenz DM, Constantinou MC. Spherical sliding isolation bearings with adaptive behavior: experimental verification. Earthq Eng Struct Dyn 2008;37(2):185–205.
[42] Tsai CS, Lin YC, Su HC. Characterization and modeling of multiple friction pendulum isolation system with numerous sliding interfaces. Earthq Eng Struct Dyn 2010;39:1463–91.
[43] Lee D, Constantinou C. Quintuple friction pendulum isolator: behavior, modeling, and validation. Earthq Spectra 2016;32(3):1607–26.
[44] Panchal VR, Jangid RS. Seismic response of structures with variable friction pendulum system. J Earthq Eng 2009;13(193–216):2009.
[45] Calvi PM, Moratti M, Calvi GM. Seismic isolation devices based on sliding between surfaces with variable friction coefficient. Earthq Spectra 2016;32(4):2291–315.
[46] Calvi PM, Timsina S. Numerical study of the seismic behaviour of variable friction base isolation systems. In: Proceedings of the 39th IABSE symposium – engineering the future. Vancouver, Canada; September 21st to 23rd 2017.
[47] Bechtold J. Earthquake proof building. US patent 845046A; Feb. 26, 1907.
[48] Hyakuda T, Saito K, Matsushita T, Tanaka N, Yoneki S, Yasuda M, Miyazaki M, Suzuki A, Sawada T. The structural design and earthquake observation of a seismic isolation building using friction pendulum system. In: Proceedings, 7th international seminar on seismic isolation, passive energy dissipation and active control of vibrations of structures. Assisi, Italy; 2001.
[49] Tsai CS, Chiang TC, Chen BJ. Shaking table tests of a full scale steel structure isolated with MFPS. In: Chen JC. (Ed.), Proceedings of the 2003 ASME pressure vessels and piping conference, seismic engineering. Cleveland, Ohio, U.S.A. 466; 20–24 July, 2003. p. 41–7.
[50] Tsai CS, Chiang TC, Chen BJ. Experimental evaluation piecewise exact solution for predicting seismic responses of spherical sliding type isolated structures. Earthq Eng Struct Dyn 2005;34(9):1027–46.
[51] Tsai CS, Chen WS, Chiang TC, Chen BJ. Component and shaking table tests for full-scale multiple friction pendulum system. Earthq Eng Struct Dyn 2006;35(11):1653–75.
[52] Dao ND, Ryan KL, Sato E, Sasaki T. Predicting the displacement of triple pendulum™ bearings in a full-scale shaking experiment using a three-dimensional element. Earthq Eng Struct Dyn 2013;42(11):1677–95.
[53] Morgan TA. The use of innovative base isolation systems to achieve complex seismic performance objectives (Ph.D. dissertation). Berkeley: Department of Civil and Environmental Engineering, University of California; 2007.
[54] Bao Y, Becker TC, Hamaguchi H. Failure of double friction pendulum bearings under pulse-type motions. Earthq Eng Struct Dyn 2017;46:715–32.
[55] Ryan KL, Soroushian S, Maragakis EM, Sato E, Sasaki T, Okazaki T. Seismic

simulation of an integrated ceiling-partition wall-piping system at E-defense, I: three-dimensional structural response and base isolation. J Struct Eng 2015;142(2):0401530.
[56] Becker TC, Mahin SA. Experimental and analytical study of the bidirectional behavior of the triple friction pendulum isolator. Earthq Eng Struct Dyn 2012;41(3):355–73.
[57] Sarlis AA, Constantinou MC. A model of triple friction pendulum bearing for general geometric and frictional parameters. Earthq Eng Struct Dyn 2016;45:1837–53.
[58] Fenz DM, Constantinou MC. Modeling triple friction pendulum bearings for response-history analysis. Earthq Spectra 2008;24(4):1011–28.
[59] Nagarajaiah S, Reinhorn AM, Constantinou MC. Nonlinear dynamic analysis of 3-D-base-isolated structures. J Struct Eng 1991;117:2035–54.
[60] Zekioglu A, Darama H, Erkus B. Performance-based seismic design of a large seismically isolated structure. Los Angeles, California: Istanbul Sabiha Gökçen International Airport Terminal Building, Arup North America Ltd; 2009.
[61] Erdik MO. State of the art on application, R&D and design rules for seismic isolation and energy dissipation for buildings, bridges and viaducts, cultural heritage and chemical plants in Turkey. In: Proceedings of the NZSEE conference; 2017.
[62] Calvi PM. Relative displacement floor spectra for seismic design of non structural elements. J Earthq Eng 2014;18(7):1037–59.
[63] Calvi PM, Sullivan TJ. Estimating floor spectra in multiple degree of freedom structures. Earthq Struct 2014;7(1):17–38.
[64] Calvi PM, Ruggiero DM. Earthquake-induced floor accelerations in base isolated structures. In: Proceedings of the 16th world conference on earthquake engineering, 16WCEE 2017. Santiago Chile; January 9th to 13th 2017.
[65] Morgan TA, Mahin SA. Achieving reliable seismic performance enhancement using multi-stage friction pendulum isolators. Earthq Eng Struct Dyn 2010;39(13):1443–61.
[66] Becker TC, Bao Y, Mahin SA. Extreme behavior in a triple friction pendulum isolated frame. Earthq Eng Struct Dyn 2017. http://dx.doi.org/10.1002/eqe.2924.
[67] Priestley MJN, Calvi GM. Strategies for repair and seismic upgrading of Bolu Viaduct 1, Turkey. J Earthq Eng 2002;6(S1):157–84.
[68] Ghasemi H, Cooper JD, Imbsen R, Piskin H, Inal F, Tiras A. November 1999 Duzce earthquake: post-earthquake investigation of the structures on the TEM. Federal highway administration. Technical report. 26 pages. Publication No. FHWA-RD-00-146; 2000.
[69] Calvi GM, Spaziante V. Reconstruction between temporary and definitive: the CASE project. Progettazione Sismica. 03/English; 2009. p. 221-50.
[70] Constantinou MC, Tsopelas P, Kim YS, Okamoto S. NCEER-Taisei corporation research program on sliding seismic isolation systems for bridges: experimental and analytical study of a friction pendulum system (FPS) Buffalo, NY: SUNY; 1993. (Technical Report NCEER-93-0020).
[71] Mosqueda G, Whittaker AS, Fenves GL, Mahin SA. Experimental and analytical studies of the friction pendulum system for the seismic protection of simple bridges Berkeley, Berkeley, CA: University of California; 2004. (Report No. UCB/EERC-2004-01).
[72] Fenz DM, Constantinou MC. Development, implementation, and verification of dynamic analysis models for multi-spherical sliding bearings Buffalo, NY: SUNY; 2008. (Technical Report MCEER-08-0018).
[73] Morgan TA, Mahin SA. The use of base isolation systems to achieve complex seismic performance objectives Berkeley, CA: PEER, University of California; 2011. (Report No. 2011/06).
[74] Ryan KL, Dao ND, Sato E, Sasaki T, Okazaki T. Aspects of isolation device behavior observed from full-scale testing of an isolated building at E-defense. In: Proceedings of the 20th analysis and computation specialty track, ASCE structures congress. Chicago, IL; 2012.
[75] Ryan KL, Soroushian S, Maragakis E, Sato E, Sasaki T, Okazaki T. Seismic simulation of an integrated ceiling-partition wall-piping system at E-defense. I: three-dimensional structural response and base isolation. ASCE J. Struct. Eng 2016;142:04015130.
[76] Roussis PC, Constantinou MC. Uplift-restraining friction pendulum seismic isolation system. Earthq Eng Struct Dyn 2006;35(5):577–93.
[77] Kaiser A, Holden C, Beavan J, Beetham D, Benites R, Celentano A, et al. The Mw 6.2 Christchurch earthquake of February 2011: preliminary report. NZ J Geol Geophys 2011;55(1):67–90.
[78] Lew M, Hudson MB. The effects of vertical ground motion on base-isolated building systems. Earthq Spectra 1999;15(2):371–5.
[79] Roussis PC. Study on the effect of uplift-restraint on the seismic response of base-isolated structures. ASCE J. Struct. Eng 135. 2009. p. 1462–71.
[80] Sumitomo Construction. Base-isolated buildings by sumitomo construction. Tokyo, Japan: Internal Report, Sumitomo Construction Co. Ltd.; 1990.
[81] Nagarajaiah S, Reinhorn AM, Constantinou MC. Experimental study of sliding isolated structures with uplift restraint. ASCE J Struct Eng 1992;118(6):1666–82.
[82] Constantinou MC, Mokha AS, Reinhorn AM. Study of sliding bearing and helical-steel-spring isolation system. ASCE J Struct Eng 1991;117(4):1257–75.
[83] Logiadis I, Zilch K, Meskouris K. Presstressed bearings in the seismic isolation of structures. Paper no. 1895, 11th WCEE. Acapulco, Mexico; 1996.
[84] Roussis PC, Constantinou MC. Experimental and analytical studies of structures seismically isolated with an uplift restraining friction pendulum system. Earthq Eng Struct Dyn 2006;35(5):595–611.
[85] Baker JW. Quantitative classification of near-fault ground motions using wavelet analysis. Bull Seismol Soc Am 2007;97(5):1486–501.
[86] Katsaras CP, Panagiotakos TB, Kolias B. Restoring capability of bilinear hysteretic seismic isolation systems. Earthq Eng Struct Dyn 2008;37(4):557–75.
[87] Ismail M, Rodellar J, Pozo F. An isolation device for near-fault ground motions. Struct Control Health Monit 2014;21(3):249–68.
[88] CBSC. California building code. Sacramento, CA: California Buildings Standards Commission; 2001.
[89] IBC. International building code. Falls Church: International Code Council; 2006.
[90] Dicleli M, Buddaram S. Effect of isolator and ground motion characteristics on the performance of seismic-isolated bridges. Earthq Eng Struct Dyn 2006;35(2):223–50.
[91] Berton S, Infanti S, Castellano MG, Hikosaka H. Self-centring capacity of seismic isolation systems. Struct Control Health Monit 2006;14(6):895–914.